FERMILAB-PUB-07-117-E

$Z\gamma$ production and limits on anomalous $ZZ\gamma$ and $Z\gamma\gamma$ couplings in $p\bar{p}$ collisions at $\sqrt{s} = 1.96$ TeV

V.M. Abazov,[35] B. Abbott,[75] M. Abolins,[65] B.S. Acharya,[28] M. Adams,[51] T. Adams,[49] E. Aguilo,[5] S.H. Ahn,[30] M. Ahsan,[59] G.D. Alexeev,[35] G. Alkhazov,[39] A. Alton,[64,*] G. Alverson,[63] G.A. Alves,[2] M. Anastasoaie,[34] L.S. Ancu,[34] T. Andeen,[53] S. Anderson,[45] B. Andrieu,[16] M.S. Anzelc,[53] Y. Arnoud,[13] M. Arov,[60] M. Arthaud,[17] A. Askew,[49] B. Åsman,[40] A.C.S. Assis Jesus,[3] O. Atramentov,[49] C. Autermann,[20] C. Avila,[7] C. Ay,[23] F. Badaud,[12] A. Baden,[61] L. Bagby,[52] B. Baldin,[50] D.V. Bandurin,[59] P. Banerjee,[28] S. Banerjee,[28] E. Barberis,[63] A.-F. Barfuss,[14] P. Bargassa,[80] P. Baringer,[58] J. Barreto,[2] J.F. Bartlett,[50] U. Bassler,[16] D. Bauer,[43] S. Beale,[5] A. Bean,[58] M. Begalli,[3] M. Begel,[71] C. Belanger-Champagne,[40] L. Bellantoni,[50] A. Bellavance,[50] J.A. Benitez,[65] S.B. Beri,[26] G. Bernardi,[16] R. Bernhard,[22] L. Berntzon,[14] I. Bertram,[42] M. Besançon,[17] R. Beuselinck,[43] V.A. Bezzubov,[38] P.C. Bhat,[50] V. Bhatnagar,[26] C. Biscarat,[19] G. Blazey,[52] F. Blekman,[43] S. Blessing,[49] D. Bloch,[18] K. Bloom,[67] A. Boehnlein,[50] D. Boline,[62] T.A. Bolton,[59] G. Borissov,[42] K. Bos,[33] T. Bose,[77] A. Brandt,[78] R. Brock,[65] G. Brooijmans,[70] A. Bross,[50] D. Brown,[78] N.J. Buchanan,[49] D. Buchholz,[53] M. Buehler,[81] V. Buescher,[21] S. Burdin,[42,¶] S. Burke,[45] T.H. Burnett,[82] C.P. Buszello,[43] J.M. Butler,[62] P. Calfayan,[24] S. Calvet,[14] J. Cammin,[71] S. Caron,[33] W. Carvalho,[3] B.C.K. Casey,[77] N.M. Cason,[55] H. Castilla-Valdez,[32] S. Chakrabarti,[17] D. Chakraborty,[52] K. Chan,[5] K.M. Chan,[55] A. Chandra,[48] F. Charles,[18] E. Cheu,[45] F. Chevallier,[13] D.K. Cho,[62] S. Choi,[31] B. Choudhary,[27] L. Christofek,[77] T. Christoudias,[43] S. Cihangir,[50] D. Claes,[67] B. Clément,[18] C. Clément,[40] Y. Coadou,[5] M. Cooke,[80] W.E. Cooper,[50] M. Corcoran,[80] F. Couderc,[17] M.-C. Cousinou,[14] S. Crépé-Renaudin,[13] D. Cutts,[77] M. Ćwiok,[29] H. da Motta,[2] A. Das,[62] G. Davies,[43] K. De,[78] P. de Jong,[33] S.J. de Jong,[34] E. De La Cruz-Burelo,[64] C. De Oliveira Martins,[3] J.D. Degenhardt,[64] F. Déliot,[17] M. Demarteau,[50] R. Demina,[71] D. Denisov,[50] S.P. Denisov,[38] S. Desai,[50] H.T. Diehl,[50] M. Diesburg,[50] A. Dominguez,[67] H. Dong,[72] L.V. Dudko,[37] L. Duflot,[15] S.R. Dugad,[28] D. Duggan,[49] A. Duperrin,[14] J. Dyer,[65] A. Dyshkant,[52] M. Eads,[67] D. Edmunds,[65] J. Ellison,[48] V.D. Elvira,[50] Y. Enari,[77] S. Eno,[61] P. Ermolov,[37] H. Evans,[54] A. Evdokimov,[73] V.N. Evdokimov,[38] A.V. Ferapontov,[59] T. Ferbel,[71] F. Fiedler,[24] F. Filthaut,[34] W. Fisher,[50] H.E. Fisk,[50] M. Ford,[44] M. Fortner,[52] H. Fox,[22] S. Fu,[50] S. Fuess,[50] T. Gadfort,[82] C.F. Galea,[34] E. Gallas,[50] E. Galyaev,[55] C. Garcia,[71] A. Garcia-Bellido,[82] V. Gavrilov,[36] P. Gay,[12] W. Geist,[18] D. Gelé,[18] C.E. Gerber,[51] Y. Gershtein,[49] D. Gillberg,[5] G. Ginther,[71] N. Gollub,[40] B. Gómez,[7] A. Goussiou,[55] P.D. Grannis,[72] H. Greenlee,[50] Z.D. Greenwood,[60] E.M. Gregores,[4] G. Grenier,[19] Ph. Gris,[12] J.-F. Grivaz,[15] A. Grohsjean,[24] S. Grünendahl,[50] M.W. Grünewald,[29] F. Guo,[72] J. Guo,[72] G. Gutierrez,[50] P. Gutierrez,[75] A. Haas,[70] N.J. Hadley,[61] P. Haefner,[24] S. Hagopian,[49] J. Haley,[68] I. Hall,[75] R.E. Hall,[47] L. Han,[6] K. Hanagaki,[50] P. Hansson,[40] K. Harder,[44] A. Harel,[71] R. Harrington,[63] J.M. Hauptman,[57] R. Hauser,[65] J. Hays,[43] T. Hebbeker,[20] D. Hedin,[52] J.G. Hegeman,[33] J.M. Heinmiller,[51] A.P. Heinson,[48] U. Heintz,[62] C. Hensel,[58] K. Herner,[72] G. Hesketh,[63] M.D. Hildreth,[55] R. Hirosky,[81] J.D. Hobbs,[72] B. Hoeneisen,[11] H. Hoeth,[25] M. Hohlfeld,[21] S.J. Hong,[30] R. Hooper,[77] S. Hossain,[75] P. Houben,[33] Y. Hu,[72] Z. Hubacek,[9] V. Hynek,[8] I. Iashvili,[69] R. Illingworth,[50] A.S. Ito,[50] S. Jabeen,[62] M. Jaffré,[15] S. Jain,[75] K. Jakobs,[22] C. Jarvis,[61] R. Jesik,[43] K. Johns,[45] C. Johnson,[70] M. Johnson,[50] A. Jonckheere,[50] P. Jonsson,[43] A. Juste,[50] D. Käfer,[20] S. Kahn,[73] E. Kajfasz,[14] A.M. Kalinin,[35] J.M. Kalk,[60] J.R. Kalk,[65] S. Kappler,[20] D. Karmanov,[37] J. Kasper,[62] P. Kasper,[50] I. Katsanos,[70] D. Kau,[49] R. Kaur,[26] V. Kaushik,[78] R. Kehoe,[79] S. Kermiche,[14] N. Khalatyan,[38] A. Khanov,[76] A. Kharchilava,[69] Y.M. Kharzheev,[35] D. Khatidze,[70] H. Kim,[31] T.J. Kim,[30] M.H. Kirby,[34] M. Kirsch,[20] B. Klima,[50] J.M. Kohli,[26] J.-P. Konrath,[22] M. Kopal,[75] V.M. Korablev,[38] B. Kothari,[70] A.V. Kozelov,[38] D. Krop,[54] A. Kryemadhi,[81] T. Kuhl,[23] A. Kumar,[69] S. Kunori,[61] A. Kupco,[10] T. Kurča,[19] J. Kvita,[8] D. Lam,[55] S. Lammers,[70] G. Landsberg,[77] J. Lazoflores,[49] P. Lebrun,[19] W.M. Lee,[50] A. Leflat,[37] F. Lehner,[41] J. Lellouch,[16] V. Lesne,[12] J. Leveque,[45] P. Lewis,[43] J. Li,[78] L. Li,[48] Q.Z. Li,[50] S.M. Lietti,[4] J.G.R. Lima,[52] D. Lincoln,[50] J. Linnemann,[65] V.V. Lipaev,[38] R. Lipton,[50] Y. Liu,[6] Z. Liu,[5] L. Lobo,[43] A. Lobodenko,[39] M. Lokajicek,[10] A. Lounis,[18] P. Love,[42] H.J. Lubatti,[82] A.L. Lyon,[50] A.K.A. Maciel,[2] D. Mackin,[80] R.J. Madaras,[46] P. Mättig,[25] C. Magass,[20] A. Magerkurth,[64] N. Makovec,[15] P.K. Mal,[55] H.B. Malbouisson,[3] S. Malik,[67] V.L. Malyshev,[35] H.S. Mao,[50] Y. Maravin,[59] B. Martin,[13] R. McCarthy,[72] A. Melnitchouk,[66] A. Mendes,[14] L. Mendoza,[7] P.G. Mercadante,[4] M. Merkin,[37] K.W. Merritt,[50] A. Meyer,[20] J. Meyer,[21] M. Michaut,[17] T. Millet,[19] J. Mitrevski,[70] J. Molina,[3] R.K. Mommsen,[44] N.K. Mondal,[28] R.W. Moore,[5] T. Moulik,[58] G.S. Muanza,[19] M. Mulders,[50] M. Mulhearn,[70] O. Mundal,[21] L. Mundim,[3] E. Nagy,[14]

M. Naimuddin,[50] M. Narain,[77] N.A. Naumann,[34] H.A. Neal,[64] J.P. Negret,[7] P. Neustroev,[39] H. Nilsen,[22] C. Noeding,[22] A. Nomerotski,[50] S.F. Novaes,[4] T. Nunnemann,[24] V. O'Dell,[50] D.C. O'Neil,[5] G. Obrant,[39] C. Ochando,[15] D. Onoprienko,[59] N. Oshima,[50] J. Osta,[55] R. Otec,[9] G.J. Otero y Garzón,[51] M. Owen,[44] P. Padley,[80] M. Pangilinan,[77] N. Parashar,[56] S.-J. Park,[71] S.K. Park,[30] J. Parsons,[70] R. Partridge,[77] N. Parua,[54] A. Patwa,[73] G. Pawloski,[80] P.M. Perea,[48] K. Peters,[44] Y. Peters,[25] P. Pétroff,[15] M. Petteni,[43] R. Piegaia,[1] J. Piper,[65] M.-A. Pleier,[21] P.L.M. Podesta-Lerma,[32,§] V.M. Podstavkov,[50] Y. Pogorelov,[55] M.-E. Pol,[2] A. Pompoš,[75] B.G. Pope,[65] A.V. Popov,[38] C. Potter,[5] W.L. Prado da Silva,[3] H.B. Prosper,[49] S. Protopopescu,[73] J. Qian,[64] A. Quadt,[21] B. Quinn,[66] A. Rakitine,[42] M.S. Rangel,[2] K.J. Rani,[28] K. Ranjan,[27] P.N. Ratoff,[42] P. Renkel,[79] S. Reucroft,[63] P. Rich,[44] M. Rijssenbeek,[72] I. Ripp-Baudot,[18] F. Rizatdinova,[76] S. Robinson,[43] R.F. Rodrigues,[3] C. Royon,[17] P. Rubinov,[50] R. Ruchti,[55] G. Safronov,[36] G. Sajot,[13] A. Sánchez-Hernández,[32] M.P. Sanders,[16] A. Santoro,[3] G. Savage,[50] L. Sawyer,[60] T. Scanlon,[43] D. Schaile,[24] R.D. Schamberger,[72] Y. Scheglov,[39] H. Schellman,[53] P. Schieferdecker,[24] T. Schliephake,[25] C. Schmitt,[25] C. Schwanenberger,[44] A. Schwartzman,[68] R. Schwienhorst,[65] J. Sekaric,[49] S. Sengupta,[49] H. Severini,[75] E. Shabalina,[51] M. Shamim,[59] V. Shary,[17] A.A. Shchukin,[38] R.K. Shivpuri,[27] D. Shpakov,[50] V. Siccardi,[18] V. Simak,[9] V. Sirotenko,[50] P. Skubic,[75] P. Slattery,[71] D. Smirnov,[55] R.P. Smith,[50] G.R. Snow,[67] J. Snow,[74] S. Snyder,[73] S. Söldner-Rembold,[44] L. Sonnenschein,[16] A. Sopczak,[42] M. Sosebee,[78] K. Soustruznik,[8] M. Souza,[2] B. Spurlock,[78] J. Stark,[13] J. Steele,[60] V. Stolin,[36] A. Stone,[51] D.A. Stoyanova,[38] J. Strandberg,[64] S. Strandberg,[40] M.A. Strang,[69] M. Strauss,[75] R. Ströhmer,[24] D. Strom,[53] M. Strovink,[46] L. Stutte,[50] S. Sumowidagdo,[49] P. Svoisky,[55] A. Sznajder,[3] M. Talby,[14] P. Tamburello,[45] A. Tanasijczuk,[1] W. Taylor,[5] P. Telford,[44] J. Temple,[45] B. Tiller,[24] F. Tissandier,[12] M. Titov,[17] V.V. Tokmenin,[35] M. Tomoto,[50] T. Toole,[61] I. Torchiani,[22] T. Trefzger,[23] D. Tsybychev,[72] B. Tuchming,[17] C. Tully,[68] P.M. Tuts,[70] R. Unalan,[65] L. Uvarov,[39] S. Uvarov,[39] S. Uzunyan,[52] B. Vachon,[5] P.J. van den Berg,[33] B. van Eijk,[33] R. Van Kooten,[54] W.M. van Leeuwen,[33] N. Varelas,[51] E.W. Varnes,[45] A. Vartapetian,[78] I.A. Vasilyev,[38] M. Vaupel,[25] P. Verdier,[19] L.S. Vertogradov,[35] M. Verzocchi,[50] F. Villeneuve-Seguier,[43] P. Vint,[43] E. Von Toerne,[59] M. Voutilainen,[67,‡] M. Vreeswijk,[33] R. Wagner,[68] H.D. Wahl,[49] L. Wang,[61] M.H.L.S Wang,[50] J. Warchol,[55] G. Watts,[82] M. Wayne,[55] G. Weber,[23] M. Weber,[50] H. Weerts,[65] A. Wenger,[22,#] N. Wermes,[21] M. Wetstein,[61] A. White,[78] D. Wicke,[25] G.W. Wilson,[58] S.J. Wimpenny,[48] M. Wobisch,[60] D.R. Wood,[63] T.R. Wyatt,[44] Y. Xie,[77] S. Yacoob,[53] R. Yamada,[50] M. Yan,[61] T. Yasuda,[50] Y.A. Yatsunenko,[35] K. Yip,[73] H.D. Yoo,[77] S.W. Youn,[53] C. Yu,[13] J. Yu,[78] A. Yurkewicz,[72] A. Zatserklyaniy,[52] C. Zeitnitz,[25] D. Zhang,[50] T. Zhao,[82] B. Zhou,[64] J. Zhu,[72] M. Zielinski,[71] D. Zieminska,[54] A. Zieminski,[54] L. Zivkovic,[70] V. Zutshi,[52] and E.G. Zverev[37]

(DØ Collaboration)

[1] *Universidad de Buenos Aires, Buenos Aires, Argentina*
[2] *LAFEX, Centro Brasileiro de Pesquisas Físicas, Rio de Janeiro, Brazil*
[3] *Universidade do Estado do Rio de Janeiro, Rio de Janeiro, Brazil*
[4] *Instituto de Física Teórica, Universidade Estadual Paulista, São Paulo, Brazil*
[5] *University of Alberta, Edmonton, Alberta, Canada, Simon Fraser University, Burnaby, British Columbia, Canada, York University, Toronto, Ontario, Canada, and McGill University, Montreal, Quebec, Canada*
[6] *University of Science and Technology of China, Hefei, People's Republic of China*
[7] *Universidad de los Andes, Bogotá, Colombia*
[8] *Center for Particle Physics, Charles University, Prague, Czech Republic*
[9] *Czech Technical University, Prague, Czech Republic*
[10] *Center for Particle Physics, Institute of Physics, Academy of Sciences of the Czech Republic, Prague, Czech Republic*
[11] *Universidad San Francisco de Quito, Quito, Ecuador*
[12] *Laboratoire de Physique Corpusculaire, IN2P3-CNRS, Université Blaise Pascal, Clermont-Ferrand, France*
[13] *Laboratoire de Physique Subatomique et de Cosmologie, IN2P3-CNRS, Universite de Grenoble 1, Grenoble, France*
[14] *CPPM, IN2P3-CNRS, Université de la Méditerranée, Marseille, France*
[15] *Laboratoire de l'Accélérateur Linéaire, IN2P3-CNRS et Université Paris-Sud, Orsay, France*
[16] *LPNHE, IN2P3-CNRS, Universités Paris VI and VII, Paris, France*
[17] *DAPNIA/Service de Physique des Particules, CEA, Saclay, France*
[18] *IPHC, Université Louis Pasteur et Université de Haute Alsace, CNRS, IN2P3, Strasbourg, France*
[19] *IPNL, Université Lyon 1, CNRS/IN2P3, Villeurbanne, France and Université de Lyon, Lyon, France*
[20] *III. Physikalisches Institut A, RWTH Aachen, Aachen, Germany*
[21] *Physikalisches Institut, Universität Bonn, Bonn, Germany*
[22] *Physikalisches Institut, Universität Freiburg, Freiburg, Germany*
[23] *Institut für Physik, Universität Mainz, Mainz, Germany*
[24] *Ludwig-Maximilians-Universität München, München, Germany*
[25] *Fachbereich Physik, University of Wuppertal, Wuppertal, Germany*
[26] *Panjab University, Chandigarh, India*

[27] *Delhi University, Delhi, India*
[28] *Tata Institute of Fundamental Research, Mumbai, India*
[29] *University College Dublin, Dublin, Ireland*
[30] *Korea Detector Laboratory, Korea University, Seoul, Korea*
[31] *SungKyunKwan University, Suwon, Korea*
[32] *CINVESTAV, Mexico City, Mexico*
[33] *FOM-Institute NIKHEF and University of Amsterdam/NIKHEF, Amsterdam, The Netherlands*
[34] *Radboud University Nijmegen/NIKHEF, Nijmegen, The Netherlands*
[35] *Joint Institute for Nuclear Research, Dubna, Russia*
[36] *Institute for Theoretical and Experimental Physics, Moscow, Russia*
[37] *Moscow State University, Moscow, Russia*
[38] *Institute for High Energy Physics, Protvino, Russia*
[39] *Petersburg Nuclear Physics Institute, St. Petersburg, Russia*
[40] *Lund University, Lund, Sweden, Royal Institute of Technology and Stockholm University, Stockholm, Sweden, and Uppsala University, Uppsala, Sweden*
[41] *Physik Institut der Universität Zürich, Zürich, Switzerland*
[42] *Lancaster University, Lancaster, United Kingdom*
[43] *Imperial College, London, United Kingdom*
[44] *University of Manchester, Manchester, United Kingdom*
[45] *University of Arizona, Tucson, Arizona 85721, USA*
[46] *Lawrence Berkeley National Laboratory and University of California, Berkeley, California 94720, USA*
[47] *California State University, Fresno, California 93740, USA*
[48] *University of California, Riverside, California 92521, USA*
[49] *Florida State University, Tallahassee, Florida 32306, USA*
[50] *Fermi National Accelerator Laboratory, Batavia, Illinois 60510, USA*
[51] *University of Illinois at Chicago, Chicago, Illinois 60607, USA*
[52] *Northern Illinois University, DeKalb, Illinois 60115, USA*
[53] *Northwestern University, Evanston, Illinois 60208, USA*
[54] *Indiana University, Bloomington, Indiana 47405, USA*
[55] *University of Notre Dame, Notre Dame, Indiana 46556, USA*
[56] *Purdue University Calumet, Hammond, Indiana 46323, USA*
[57] *Iowa State University, Ames, Iowa 50011, USA*
[58] *University of Kansas, Lawrence, Kansas 66045, USA*
[59] *Kansas State University, Manhattan, Kansas 66506, USA*
[60] *Louisiana Tech University, Ruston, Louisiana 71272, USA*
[61] *University of Maryland, College Park, Maryland 20742, USA*
[62] *Boston University, Boston, Massachusetts 02215, USA*
[63] *Northeastern University, Boston, Massachusetts 02115, USA*
[64] *University of Michigan, Ann Arbor, Michigan 48109, USA*
[65] *Michigan State University, East Lansing, Michigan 48824, USA*
[66] *University of Mississippi, University, Mississippi 38677, USA*
[67] *University of Nebraska, Lincoln, Nebraska 68588, USA*
[68] *Princeton University, Princeton, New Jersey 08544, USA*
[69] *State University of New York, Buffalo, New York 14260, USA*
[70] *Columbia University, New York, New York 10027, USA*
[71] *University of Rochester, Rochester, New York 14627, USA*
[72] *State University of New York, Stony Brook, New York 11794, USA*
[73] *Brookhaven National Laboratory, Upton, New York 11973, USA*
[74] *Langston University, Langston, Oklahoma 73050, USA*
[75] *University of Oklahoma, Norman, Oklahoma 73019, USA*
[76] *Oklahoma State University, Stillwater, Oklahoma 74078, USA*
[77] *Brown University, Providence, Rhode Island 02912, USA*
[78] *University of Texas, Arlington, Texas 76019, USA*
[79] *Southern Methodist University, Dallas, Texas 75275, USA*
[80] *Rice University, Houston, Texas 77005, USA*
[81] *University of Virginia, Charlottesville, Virginia 22901, USA*
[82] *University of Washington, Seattle, Washington 98195, USA*

(Dated: May 9, 2007)

We present a study of $ee\gamma$ and $\mu\mu\gamma$ events using 1109 (1009) pb^{-1} of data in the electron (muon) channel, respectively. These data were collected with the D0 detector at the Fermilab Tevatron $p\bar{p}$ Collider at $\sqrt{s} = 1.96$ TeV. Having observed 453 (515) candidates in the $ee\gamma$ ($\mu\mu\gamma$) final state, we measure the $Z\gamma$ production cross section for a photon with transverse energy $E_T > 7$ GeV,

separation between the photon and leptons $\Delta R_{\ell\gamma} > 0.7$, and invariant mass of the di-lepton pair $M_{\ell\ell} > 30$ GeV/c^2, to be 4.96 ± 0.30 (stat. + syst.) ± 0.30 (lumi.) pb, in agreement with the standard model prediction of 4.74 ± 0.22 pb. This is the most precise $Z\gamma$ cross section measurement at a hadron collider. We set limits on anomalous trilinear $Z\gamma\gamma$ and $ZZ\gamma$ gauge boson couplings of $-0.085 < h_{30}^{\gamma} < 0.084$, $-0.0053 < h_{40}^{\gamma} < 0.0054$ and $-0.083 < h_{30}^{Z} < 0.082$, $-0.0053 < h_{40}^{Z} < 0.0054$ at the 95% C.L. for the form-factor scale $\Lambda = 1.2$ TeV.

PACS numbers: 12.15.Ji, 13.40.Em, 13.85.Qk

The analysis of vector boson self-interactions provides an important test of the gauge sector of the standard model (SM). At the tree level, a Z boson cannot couple to a photon. Various extensions of the SM [1] predict large (anomalous) values of the trilinear couplings $ZZ\gamma$ and $Z\gamma\gamma$ that result in an excess of photons with high transverse energy (E_T) compared with the SM prediction. Consequently, the cross section for $Z\gamma$ production will be higher than that predicted by the SM. An observation of either an enhancement of the cross section or an excess of photons with high E_T would indicate new physics [2].

Previous studies of Z boson production in association with a photon were made at the Fermilab Tevatron $p\bar{p}$ Collider by the CDF [3] and D0 [4, 5] collaborations, and at the LEP collider by the ALEPH [6], DELPHI [7], L3 [8], and OPAL [9] collaborations. The combined LEP results are available in Ref. [10]. All results are consistent with SM predictions.

In this work, we present a measurement of the $Z\gamma$ cross section and a search for anomalous trilinear $ZZ\gamma$ and $Z\gamma\gamma$ couplings. We follow the framework of Ref. [11], where the $ZV\gamma$ ($V = Z$, γ) couplings are assumed only to be Lorentz and gauge invariant. Such $ZV\gamma$ couplings can be parameterized by two CP-violating (h_1^V and h_2^V) and two CP-conserving (h_3^V and h_4^V) complex parameters. Partial wave unitarity is ensured by using a form-factor parameterization that causes the coupling to vanish at high center-of-mass energy $\sqrt{\hat{s}}$: $h_i^V = \frac{h_{i0}^V}{(1+\hat{s}/\Lambda^2)^n}$. Here, Λ is a form-factor scale, h_{i0}^V are the low-energy approximations of the couplings, and n is the form-factor power. In accordance with Ref. [11], we set $n = 3$ for $h_{1,3}^V$ and $n = 4$ for $h_{2,4}^V$. In this analysis, we set limits only on the real parts of the anomalous couplings, $Re(h_i^V)$. For convenience we omit the notation Re and refer to symbols h_i^V as the real parts of the couplings throughout the text.

The signal sample is selected by requiring a final state that consists of a photon and a pair of either muon or electron candidates. The e^+e^- and $\mu^+\mu^-$ pairs can be produced either by the decay of an on-shell Z boson or via a virtual Z boson or a photon through the Drell-Yan production mechanism. We do not distinguish between these two processes. The photon can be produced by final state radiation (FSR) off both charged leptons or by one of the partons in the p or $\bar{p}$ through initial state radiation (ISR). We collectively refer to all these processes as $Z\gamma$ production.

Data for this analysis were collected with the D0 detector at the Tevatron Collider at $p\bar{p}$ center-of-mass energy $\sqrt{s} = 1.96$ TeV between October 2002 and February 2006. The integrated luminosity is 1109±68 (1009±62) pb^{-1} [12] for the electron (muon) final state.

The D0 detector [13] is a multi-purpose detector designed to operate at the high luminosity Tevatron collider. The main components of the detector are an inner tracker, liquid-argon/uranium calorimeters, and a muon system. The inner tracker consists of a silicon microstrip tracker (SMT) and a central fiber tracker (CFT), located in a 2 T superconducting solenoidal magnet and capable of providing measurements up to pseudorapidities of $|\eta| \approx 3.0$ and $|\eta| \approx 1.8$, respectively. The calorimeter is divided into three sections which cover a wide range of pseudorapidities: the central calorimeter (CC) for $|\eta| < 1.1$ and two end calorimeters (EC) which extend coverage to $|\eta| \approx 4$. The calorimeters are longitudinally segmented into electromagnetic (EM) and hadronic sections. The muon system is the outer subsystem of the D0 detector. It includes tracking detectors, scintillation trigger counters, and a 1.8 T toroidal magnet, and has coverage up to $|\eta| \approx 2.0$. Luminosity is measured using plastic scintillator arrays located in front of the EC cryostats and covering $2.7 < |\eta| < 4.4$.

The D0 detector utilizes a three-level (L1, L2, and L3) trigger system. In the electron decay channel, we require events to satisfy one of the high-E_T electron triggers. At L1, these triggers require an event to have an energy deposit of more than 10 GeV in the EM section of the calorimeter. At L3, additional requirements are imposed on the fraction of energy deposited in the EM calorimeter and the shape of the energy deposition. Single high-E_T triggers are about 99% efficient for selecting a pair of electrons from $Z \to ee$ decays. In the muon decay channel, we require events to satisfy single and di-muon triggers. The single muon trigger requires hits in the muon system scintillators and a match with a track at L1, and, in portions of the data set, also requires spatially-matched hits in the muon tracking detectors. At L2, muon track segments are reconstructed and a p_T requirement is imposed. At L3, some of the triggers also require a reconstructed track in the inner tracker with transverse momentum (p_T) greater than 10 GeV/c. Di-muon trigger requirements on individual muon candidates are less stringent than those of single muon triggers, but they require two muon candidates at L1. The muon trigger

definitions were changing over the period of time when the data set was collected, therefore, to calculate trigger efficiencies we divide the data into several subsets and estimate the trigger efficiency separately for each subset. As determined from the Monte Carlo simulation, the resulting overall muon trigger efficiency is 68% to select a pair of muons from $Z \to \mu\mu$ decays.

We select Z boson candidates in the electron channel by requiring two isolated energy deposits (electromagnetic clusters) corresponding to $E_T > 15$ GeV in the calorimeter with at least 90% of their energy deposited in the EM calorimeter, have a shower shape consistent with that of an electron, have matched tracks, and form an invariant mass $M_{ee} > 30$ GeV/c^2. To satisfy single EM trigger requirements, we require at least one of the electron candidates to have $E_T > 25$ GeV. As $Z\gamma$ production yields leptons predominantly at small pseudo-rapidity (η) and tracking reconstruction efficiency decreases rapidly with η in the endcap region, we require at least one electron candidate to be reconstructed in the central region of the calorimeter with $|\eta| < 1.1$. The other electron can be reconstructed either in the central region (CC-CC topology) or in the endcap (CC-EC topology).

To select $Z \to \mu\mu$ events we require the event to have a pair of muon candidates each with $p_T > 15$ GeV/c, reconstructed within the muon system acceptance, that match to central tracks. At least one of the muon candidates must have $p_T > 20$ GeV/c. To suppress the background from hadronic $b\bar{b}$ production, with b quarks decaying semi-leptonically, we require muon candidates to be isolated from other activity in both the central tracker and the calorimeter. The background from cosmic ray muons is suppressed by rejecting muon tracks that are inconsistent with being produced at the interaction point. This background is further reduced by rejecting muon candidates that are reconstructed back-to-back with an opening angle $\Delta\alpha_{\mu\mu} = |\Delta\phi_{\mu\mu} + \Delta\theta_{\mu\mu} - 2\pi| < 0.05$. Both muon candidates must be consistent with being produced at the same vertex, i.e., they must originate within 2 cm from each other. The event is also rejected if the invariant mass of the muon pair $M_{\mu\mu} < 30$ GeV/c^2.

Each event must have at least one photon candidate identified in the central region of the D0 detector ($|\eta| < 1.1$) that deposits at least 90% of its energy in the EM calorimeter and has a shower shape consistent with that of a photon. The photon candidate E_T must exceed 7 GeV, and it must be separated from both leptons by 0.7 in $\Delta R = \sqrt{(\phi_\ell - \phi_\gamma)^2 + (\eta_\ell - \eta_\gamma)^2}$. As electrons are not a significant source of a background to photon candidates in $Z\gamma$ final state, we do not require an anti-track match to the photon candidate. To reduce contamination from EM-like jets, we require the photon to be isolated from reconstructed tracks in the annulus of $0.05 < \Delta R < 0.4$ – the scalar sum of all the momenta of the tracks in this annulus must be below 1.5 GeV/c. These track isolation requirements result in overall improvement (about 8%) of photon identification efficiency and smaller systematic uncertainty due to simulation of converted photons than that employed in the previous analysis [5]. The $Z(\gamma)$ candidate events that pass all the selection criteria are collectively called the signal sample.

We determine the electron and muon identification efficiencies using the tag and probe method [14] on $Z \to \ell\ell$ data samples. In the electron channel, we parameterize the efficiency as a function of η, E_T, and z-coordinate of the interaction vertex. The reconstruction and trigger efficiencies are then calculated using the signal Monte Carlo samples processed with the GEANT-based [15] D0 simulation package. The efficiency to reconstruct a pair of electrons is estimated to be $(64.6 \pm 2.2)\%$ for the CC-CC topology and $(50.8 \pm 2.4)\%$ for the CC-EC topology, resulting in the combined reconstruction and trigger efficiency in the electron channel to be $(64.0 \pm 2.3)\%$ for the CC-CC topology and $(50.3 \pm 2.4)\%$ for the CC-EC topology, respectively. The efficiency to reconstruct a pair of muons is measured to be $(78.8 \pm 1.6)\%$, resulting in $(53.4 \pm 1.2)\%$ combined reconstruction and trigger efficiency. The main contribution to the uncertainty in both channels is from the lepton identification uncertainty. As no clean high-E_T photon sample exists, we measure the photon identification efficiency using photon Monte Carlo simulation. The quality of how well Monte Carlo simulation describes EM objects in data is studied on $Z \to ee$ candidate data sample. The data and Monte Carlo electron E_T distributions agree at $(99 \pm 1)\%$. We normalize the photon efficiency by this number to correct for data-Monte Carlo simulation difference. The photon identification efficiency is parameterized as a function of E_T; it is measured to rise from $\sim 87\%$ at a photon E_T of 7 GeV to $\sim 95\%$ for photons with E_T above 75 GeV.

The main background to the $Z\gamma$ process is Z+jet production, where an EM-like jet is misidentified as a photon. The procedure is to count the number of jets in Z+jet events that satisfy "loose" EM identification criteria and scale that by the probability for a jet that passes "loose" EM requirements to also pass the rest of the EM identification criteria. This is slightly complicated by the presence of real photons in the jet data. We correct for the contribution due to real photons by removing them from the sample when determining the jet misidentification rate. In detail, to estimate the Z+jet background to the $Z\gamma$ process, we loosen the shower shape and track isolation requirements on the photon candidates. If such "loose" photon candidates' E_T spectrum is denoted as $dN_{\rm EM}/E_T$ and that for photon candidates is denoted as dN_γ/E_T, then the number of Z+jet background events in the signal sample, $N_{Z+\text{jet bkg}}$, can be determined by using the following formula:

$$N_{Z+\text{jet bkg}} = \int \frac{f}{\epsilon_\gamma - f}\left(\epsilon_\gamma \frac{dN_{\rm EM}}{E_T} - \frac{dN_\gamma}{E_T}\right) dE_T, \quad (1)$$

where ϵ_γ is the E_T-dependent photon identification ef-

ficiency (measured with respect to the "loose" photon identification criteria), and f is the E_T-dependent probability of a jet that satisfies "loose" EM criteria to pass shower shape requirements. This probability is determined from a data sample that has at least one high-quality jet candidate that satisfies the D0 jet trigger requirement. Such data are primarily due to multijet production, and any photon-like cluster is likely to be a misidentified jet. The E_T-dependent probability is measured as the ratio of all EM clusters that pass all photon identification criteria to the total number of "loose" photon candidates reconstructed in the sample. There are real photons in the sample from direct photon production (γ+jet processes), leading to an enhancement in the misidentification rate for photons with high E_T. This contribution is removed by taking into account the relative cross sections of multijet and γ+jet processes and using the γ+jet Monte Carlo simulation. The misidentification rate is about 20% at E_T of 7 GeV and rapidly decreases to about 0.5% for $E_T > 60$ GeV. The background suppression was improved, compared with the previous analysis, by improving the performance of the D0 track reconstruction software and by increasing track-isolation requirements imposed on the photon candidate.

We predict 29.5 ± 4.8(stat.) $\pm$ 3.1(syst.) background events for the CC-CC topology and 25.7 ± 3.8(stat.) $\pm$ 2.5(syst.) background events for the CC-EC topology in the electron channel. Thus, the background in the combined electron channel is estimated to be 55.2 ± 6.1(stat.) $\pm$ 5.6(syst.) events, while that in the muon channel is 61.3 ± 6.5(stat.) $\pm$ 6.2(syst.). Backgrounds from other processes are estimated to be negligible.

We estimate the acceptance and efficiencies of the event selection criteria using Monte Carlo samples produced with the leading-order (LO) $Z\gamma$ generator [11] and the simulation of the D0 detector. The CTEQ6L1 [16] parton distribution function (PDF) set is used. The uncertainty on the acceptance due to the choice of the PDF set is estimated to be 4.7% following the procedures described in Ref. [16]. We estimate the product of overall reconstruction efficiency and geometrical acceptance of selection criteria to be 0.049 ± 0.003 for the CC-CC topology and 0.026 ± 0.002 for the CC-EC topology in the electron channel and 0.086 ± 0.005 in the muon channel.

After applying all of the event selection criteria, we observe 453 (308 CC-CC and 145 CC-EC) $ee\gamma$ events, while the SM predicts 393.4 ± 37.6 (255.7 CC-CC and 137.7 CC-EC) signal events with 55.2 ± 8.3 background events. In the muon channel, we observe 515 events compared to an estimated 410.5 ± 35.9 SM $\mu\mu\gamma$ events and 61.3 ± 9.0 background events. Uncertainty due to the PDF choice is the main contributor to the SM signal uncertainty. A major contribution to the uncertainty in the number of background events is the uncertainty in the measurement of the jet misidentification rate.

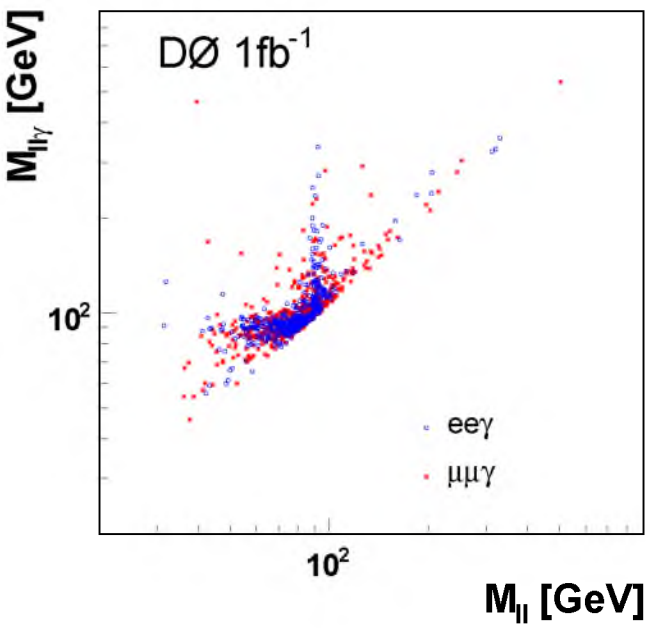

FIG. 1: Di-lepton+photon *vs.* di-lepton mass of $Z\gamma$ candidate events. Masses of candidates in the electron channel are shown as open circles, while those in the muon mode are shown as stars.

The invariant mass of di-lepton and photon versus di-lepton invariant mass scatter plot is presented in Fig. 1. The structure of this distribution reflects the three processes through which the final states can be produced. Following from the kinematics, the ISR events have two leptons from on-shell Z boson decay with $M_{\ell\ell} \approx M_Z$ and a photon, emitted by one of the interacting partons, resulting in $M_{\ell\ell\gamma} > M_Z$, and hence the ISR events populate the vertical band. The on-shell Z boson FSR events cluster along the horizontal band at $M_{\ell\ell\gamma} \approx M_Z$ and have $M_{\ell\ell} < M_Z$. Drell-Yan events populate the diagonal band with $M_{\ell\ell} \approx M_{\ell\ell\gamma}$. The di-lepton and three-body mass distributions from data as well as the SM prediction with the background overlaid are shown in Fig. 2.

The measured value of the combined $\ell\ell\gamma$ cross section times the branching ratio for $Z(\gamma) \to \ell\ell\gamma$ for a photon with $E_T > 7$ GeV, separation between the photon and leptons $\Delta R_{\ell\gamma} > 0.7$, and invariant mass of the di-lepton pair $M_{\ell\ell} > 30$ GeV/c^2, is 4.96 ± 0.30(stat. + syst.) $\pm$ 0.30(lumi.) pb. The combined statistical and systematic uncertainties contribute to the first uncertainty term, and the second uncertainty term is due solely to the uncertainty of the luminosity measurement. The measured cross section value agrees well with the theoretical prediction of 4.74 ± 0.22 pb, calculated using the NLO event generator [17].

The E_T distribution of the photon candidates in data, compared with the background and SM prediction is il-

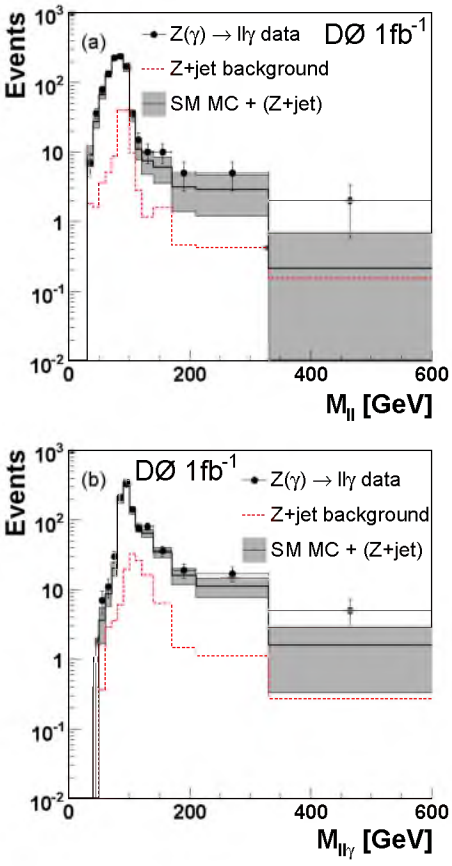

FIG. 2: (a) Di-lepton mass and (b) di-lepton+photon mass distributions of $\ell\ell\gamma$ data (solid circles), Z+jet background (dashed line histogram), and the standard model plus background (solid line histogram). The shaded bands illustrate the systematic and statistical uncertainty on the Monte Carlo and Z+jet prediction. The Monte Carlo distribution is normalized to the luminosity.

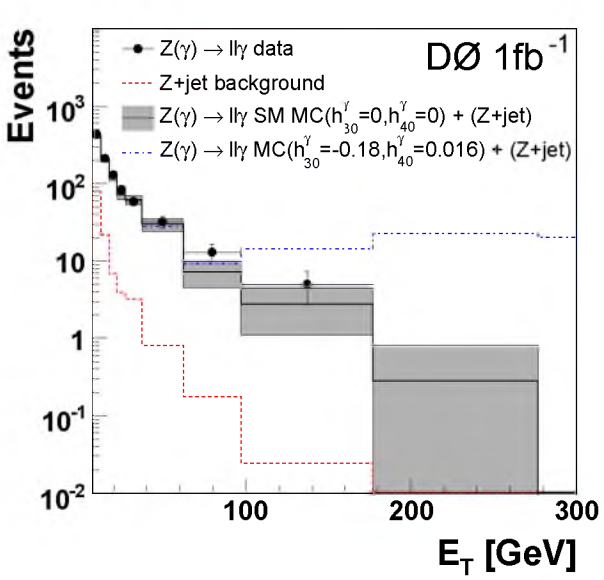

FIG. 3: Photon E_T spectrum for $\ell\ell\gamma$ data (solid circles), Z+jet background (dashed line histogram), and Monte Carlo signal plus background for the SM prediction (solid line histogram) and for the expected distribution when $h_{30}^{\gamma} = -0.18$ and $h_{40}^{\gamma} = 0.016$ (dash-dot line histogram). The shaded bands illustrate the systematic and statistical uncertainty on the SM Monte Carlo and Z+jet prediction. The Monte Carlo distributions are normalized to the luminosity.

lustrated in Fig. 3. The E_T distribution expected from a new physics process with anomalous couplings is also shown as a dashed line. As the measured $Z\gamma$ cross section agrees well with the SM expectation, we set limits on the real parts of the trilinear gauge $ZZ\gamma$ and $Z\gamma\gamma$ couplings by comparing the photon candidate E_T distribution, measured in data, with the expected E_T distribution from anomalous $Z\gamma$ production for a given set of $ZZ\gamma$ and $Z\gamma\gamma$ coupling values.The simulation of anomalous $Z\gamma$ production is obtained using the leading-order $Z\gamma$ Monte Carlo generator [11]. We take into account the next-to-leading order effects by correcting the leading-order photon E_T distributions, both for the SM and the anomalous $Z\gamma$ processes, with the E_T-dependent K-factor obtained from the next-to-leading-order $Z\gamma$ generator [17].

In this analysis, we set limits on the real parts of CP-conserving anomalous trilinear couplings h_{30}^V and h_{40}^V for the form-factor scale $\Lambda = 1.2$ TeV. This choice of Λ is not arbitrary, and is the highest possible for this current data sample that still ensures the limits not to exceed the unitarity boundaries. We generate samples of $Z\gamma$ events varying the values of the anomalous couplings h_{30}^V and h_{40}^V, and for each value we compare the photon E_T spectrum from data with that from the simulation with the background component overlaid.

The likelihood of the data-Monte Carlo simulation match is calculated assuming Poisson statistics for the signal (both in the data and MC samples) and the background. All systematic uncertainties on backgrounds, efficiencies, and luminosity are taken to be Gaussian. The two-dimensional 95% C.L. limits are shown in Fig. 4. We also measure 95% C.L. limits on individual anomalous couplings by setting the other couplings to their SM value (zero). These limits are presented in Table I and shown in Fig. 4 with crosses. The limit on h_{10}^V (h_{20}^V) is the same within the precision of this measurement as the limit on h_{30}^V (h_{40}^V) [17]. We also obtain one dimensional 95% C.L. limits on the real parts of CP-conserving anomalous couplings for the form-factor scale $\Lambda = 1$ TeV to be $-0.111 < h_{30}^{\gamma} < 0.113$, $-0.0078 < h_{40}^{\gamma} < 0.0079$ and $-0.109 < h_{30}^{Z} < 0.110$, $-0.0077 < h_{40}^{Z} < 0.0078$. This is roughly a factor of two improvement compared to the results obtained in Ref. [5]. It should be noted that Ref. [5] could not use form-factor scale $\Lambda = 1.2$ TeV because the resulting anomalous coupling limits would have been outside the contours provided by the S-matrix

TABLE I: Summary of the 95% C.L. limits on the real parts of the anomalous couplings for a form-factor scale of $\Lambda = 1.2$ TeV. Limits are set by allowing only one coupling to vary; the other is fixed to its SM value.

$-0.085 < h_{30}^{\gamma} < 0.084$	$-0.0053 < h_{40}^{\gamma} < 0.0054$	$(h_i^Z = 0)$
$-0.083 < h_{30}^{Z} < 0.082$	$-0.0053 < h_{40}^{Z} < 0.0054$	$(h_i^\gamma = 0)$

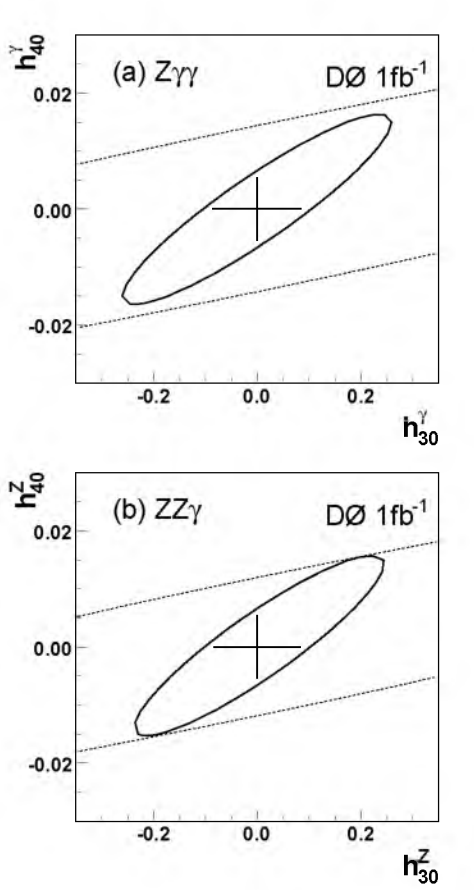

FIG. 4: The 95% C.L. two-dimensional contour (ellipse) and one-dimensional (ticks on the cross) exclusion limits for the real parts of the CP-conserving (a) $Z\gamma\gamma$ and (b) $ZZ\gamma$ couplings for $\Lambda = 1.2$ TeV. Dashed lines illustrate the unitarity constraints. Both $Z\gamma\gamma$ and $ZZ\gamma$ limits are within the unitarity boundaries.

unitarity.

In this study we analyzed a sample of 968 $\ell\ell\gamma$ events, consistent with $Z\gamma$ production. These data correspond to about 1 fb^{-1} of integrated luminosity, roughly three times more than what was used in the previous D0 analysis [5]. This current study also takes advantage of numerous improvements in the detector simulation, particle identification, and signal modeling. The cross section of the $Z\gamma$ process is measured to be $4.96 \pm 0.30(\text{stat.} + \text{syst.}) \pm 0.30(\text{lumi.})$ pb. This value is consistent with the SM, and is the most precise measurement of a $Z\gamma$ cross section at a hadron collider. The observed photon E_T distribution, as well as other kinematic parameters, do not indicate new physics beyond the SM, allowing us to set limits on the real parts of the anomalous $Z\gamma\gamma$ and $ZZ\gamma$ couplings. The one dimensional limits at the 95% C.L. for CP-conserving couplings are $-0.085 < h_{30}^{\gamma} < 0.084$, $-0.0053 < h_{40}^{\gamma} < 0.0054$ and $-0.083 < h_{30}^{Z} < 0.082$, $-0.0053 < h_{40}^{Z} < 0.0054$ for $\Lambda = 1.2$ TeV. Limits on the CP-violating couplings are the same as those on the corresponding CP-conserving couplings within the quoted precision. These new limits represent a significant improvement over previous results and the limits on h_{40}^{V} are the most stringent to date.

We thank the staffs at Fermilab and collaborating institutions, and acknowledge support from the DOE and NSF (USA); CEA and CNRS/IN2P3 (France); FASI, Rosatom and RFBR (Russia); CAPES, CNPq, FAPERJ, FAPESP and FUNDUNESP (Brazil); DAE and DST (India); Colciencias (Colombia); CONACyT (Mexico); KRF and KOSEF (Korea); CONICET and UBACyT (Argentina); FOM (The Netherlands); PPARC (United Kingdom); MSMT (Czech Republic); CRC Program, CFI, NSERC and WestGrid Project (Canada); BMBF and DFG (Germany); SFI (Ireland); The Swedish Research Council (Sweden); Research Corporation; Alexander von Humboldt Foundation; and the Marie Curie Program.

[*] Visitor from Augustana College, Sioux Falls, SD, USA.
[¶] Visitor from The University of Liverpool, Liverpool, UK.
[§] Visitor from ICN-UNAM, Mexico City, Mexico.
[‡] Visitor from Helsinki Institute of Physics, Helsinki, Finland.
[#] Visitor from Universität Zürich, Zürich, Switzerland.

[1] D. Choundhury *et al.*, Int. J. Mod. Phys. A **16**, 4891 (2001).
[2] G. J. Gounaris, J. Layssac, and F. M. Renard, Phys. Rev. D **67**, 013012 (2003).
[3] CDF Collaboration, D. Acosta *et al.*, Phys. Rev. Lett. **94**, 041803 (2005); CDF Collaboration, F. Abe *et al.*, Phys. Rev. Lett. **74**, 1941 (1995).
[4] DØ Collaboration, B. Abbott *et al.*, Phys. Rev. D **57**, 3817 (1998); DØ Collaboration, S. Abachi *et al.*, Phys. Rev. Lett. **78**, 3640 (1997); DØ Collaboration, S. Abachi *et al.*, Phys. Rev. Lett. **75**, 1028 (1995).
[5] DØ Collaboration, V. Abazov *et al.*, Phys. Rev. Lett. **95**, 051802 (2005).
[6] ALEPH Collaboration, ALEPH 2001-061 (July 2001), CERN-CONF-2001-041.
[7] DELPHI Collaboration, P. Abreu *et al.*, Phys. Lett. B **380**, 471 (1996).
[8] L3 Collaboration, P. Acciarri *et al.*, Phys. Lett. B **346**, 190 (1995); L3 Collaboration, P. Achard *et al.*, Phys. Lett. B **597**, 119 (2004).
[9] G. Abbiendi *et al.*, Eur. Phys. J. C **32**, 303 (2003).
[10] W.-M. Yao *et al.*, J. Phys. G: Nucl. Part. Phys. **33** (2006).

[11] U. Baur and E. Berger, Phys. Rev. D **47**, 4889 (1993).
[12] T. Edwards *et al.*, FERMILAB-TM-2278-E (2004).
[13] DØ Collaboration, V. Abazov *et al.*, Nucl. Instrum. Methods A **565**, 463 (2006).
[14] DØ Collaboration, V. Abazov *et al.*, "*$t\bar{t}$ cross section using kinematic characteristics of lepton+jet events*", in preparation.
[15] R. Brun and F. Carminati, CERN Program Library Long Writeup W5013, 1993 (unpublished).
[16] CTEQ Collaboration, J. Pumplin *et al.*, JHEP **0207**, 012 (2002).
[17] U. Baur, T. Han, and J. Ohnemus, Phys. Rev. D **57**, 2823 (1998).